A R C H I V E S O F M E T A L L U R G Y A N D M A T E R I A L S
Volume 58 2013 Issue 4
DOI: 10.2478/amm-2013-0151

M. ROSIAK*

THE RESULTS OF CONSOLIDATION OF SINTERS BEING DEFORMED UNDER COMPLEX LOADING CONDITION

EFEKT ZAGĘSZCZANIA SPIEKÓW ODKSZTAŁCANYCH W ZŁOŻONYM STANIE OBCIĄŻENIA

The paper deals with the analysis of the possible application of deformation to sinters under uniaxial compression combined with oscillatory torsion. The main problem of the technology relating to the manufacturing of heavy duty machine components using metal powders is associated with the difficulty to obtain sufficiently high, homogeneously distributed densities across the product volume. The tests were carried out using a test stand allowing the deformation under uniaxial compression combined with torsion. The sintered test specimens were made from the NC 100.24 iron powder. The fabricated sintered test specimens were subject to deformation under the uniaxial compression combined with oscillatory torsion, at three different torsion angle values $\alpha = \pm 3^0; \pm 5^0; \pm 7^0$ respectively. In order to investigate the effect of different torsion frequencies, each test was made at each torsion angle α for at three different frequencies f = 1 Hz; 0.71Hz; 0.32Hz, respectively, and at the same compression velocity. The results obtained allow to conclude that the application of the combined uniaxial compression and oscillatory torsion (for the preset value of draft) during the tests permitted to obtain the average density of the sinters greater than that obtainable in the case of only unconstrained uniaxial compression. The effect of increased density was enhanced by both the additional torsion-induced deformation, and the tangential stress which would promote the closing of pores.

Keywords: deformation path, oscillatory torsion, deformation of the sinters, density of the sinter, consolidation of sinters, porosity distribution

W pracy analizowano możliwość zastosowania odkształcania spieków w warunkach jednoosiowego ściskania z równoczesnym oscylacyjnym skręcaniem. Głównym problemem technologii wytwarzania elementów maszyn z proszków metali, pracujących w warunkach wysokich obciążeń, jest uzyskiwanie dużej gęstości przy jednorodnym jej rozkładzie w objętości wyrobu. Próby przeprowadzono na stanowisku, pozwalającym na odkształcanie w warunkach jednoosiowego ściskania z równoczesnym skręcaniem. Wsad do wykonania próbek spiekanych stanowił proszek żelaza NC 100.24. Uzyskane próbki spiekane odkształcano w próbie jednoosiowego ściskania z równoczesnym oscylacyjnym skręcaniem w trzech wariantach kąta skręcenia $\alpha = \pm 30; \pm 50; \pm 70$. Dla uwzględnienia wpływu częstotliwości skręceń, dla każdego wariantu kąta skręcenia α, próby realizowano w trzech wariantach częstotliwości f=1Hz; 0,71Hz; 0,32Hz i przy jednakowej prędkości ściskania. Uzyskane wyniki pozwoliły stwierdzić, że zastosowanie w czasie próby jednoosiowego ściskania (do zadanej wielkości gniotu) równoczesnego skręcania oscylacyjnego, pozwala uzyskać średnią gęstość spieku większą niż w przypadku zastosowania tylko jednoosiowego ściskania swobodnego. Elementem sprzyjającym wzrostowi gęstości jest dodatkowe odkształcenie wywołane skręcaniem oraz naprężenie styczne sprzyjające efektywniejszemu zamykaniu porów.

1. Introduction

Unlike solid materials, sintered porous materials have a specific, different structure. The essence of that structural difference is the presence of material discontinuities, referred to as porosity, which is the consequence of the following factors - batch (metal powder) properties, consolidation conditions, sintering parameters and the history of further processing of sinters during plastic working operations. Final properties of solid materials are a consequence of the batch properties and the nature of the effect of the plastic deformation occurring on the individual stages of the given technology (under the conditions of a constant density across the volume of the product). In case of sintered powders, the list of parameter dependencies specified above includes also a strong dependence on the nature of discontinuities across the porosity profile. The distribution and the differentiation of discontinuities across local areas of porosity determine the properties of the final product, what should be kept in mind when developing the technology of products made of metal powders. Cold working of solid metal alloys requires the knowledge of their technological properties described by the functions σ_p (changes in yield stress) and ε_g (strain limit) that reflect the effect of such parameters as ε (strain), $\dot{\varepsilon}$ (strain velocity), T (temperature), h_ε (the history of deformations), and k_σ (stress status indicator). Technological properties of solid alloys do not depend on the batch density, because this parameter is assumed to be constant (in a macroscopic scale) throughout the cold deformation process.

* CHAIR OF MATERIALS SCIENCE AND CHIPLESS TECHNOLOGIES, FACULTY OF MECHANICS, OPOLE UNIVERSITY OF TECHNOLOGY, 76 PRÓSZKOWSKA STR., 45-758 OPOLE, POLAND

Technological properties of porous metal alloys depend on the effect of the same parameters, which additionally affect the evolution of changes in the porosity quantity and distribution across the volume of the batch, the nature of the course of consolidation, and the magnitude and distribution of the final properties of the product.

Currently, investigations are being performed to study the effect of unconventional methods of deformation of solid materials on the changes in their internal structure, and consequently on the final properties of the material after deformation [1,3,4,5,6,7]. Up to now, the conventional methods of the assessment of the deformation effect on the internal structure of sinters have been used, being the methodology operations limited to the use of "pure" states of loads, such as compression or torsion. Application of "pure" states of loads in the deformation of materials appears to be favourable for the deformation heterogeneity across the material volume, whilst in the case of porous materials, significantly affects the heterogeneity of shape, magnitude and distribution of pores [11], causing a large variation in the density of the product, what is in some cases especially undesirable, as it leads to a considerable reduction of the mechanical properties in local areas. The effective shifting of the performed simultaneously oscillatory and torsional motion onto the material during the unconstrained compression test [1,12] guarantees the material deformation in the conditions of the complex and changing loads, whilst in the case of cold working processes, it significantly reduces the increase of the consolidation curve [2,4].

2. Course of the investigations

2.1. Material used in the investigations

The sintered test specimens were made of the Höganäs NC 100.24 grade iron powder produced through the reduction of iron oxide (ore) in the solid state. The various chemical compositions of the powder used in the manufacture of sinters are shown in Table 1, whilst the values of granularity of the powder are shown in Table 2.

TABLE 1
Chemical composition of the powder used to fabricate the sinters

Chemical element	Type of powder
	NC 100.24
	Content of chemical element %
H_2 loss	0.21
C	<0.01
Ni	
Cu	
Mo	
Fe	The rest

The NC 100.24 iron powder is one of the most popular materials in powder metallurgy. Due to its sponge-like structure, NC 100.24 allows to obtain favourable stress distribution which enables to manufacture of compacts characterised by either low or high degree of concentration. High compactibility of the NC 100.24 iron is fundamental for the wide use of this material to make powder metallurgy parts.

TABLE 2
Grain size of the powder used to fabricate the sinters

Grain size in μm	Type of powder
	NC 100.24
	Fraction in %
+212	0.0
180-212	–
150-180	–
150-212	1.0
106-150	81.0
75-106	
45-75	
- 45	18.0

2.2. Technology of production of sinters

The batch for consolidation was prepared through mixing of iron powder with 0.7% of zinc stearate (this latter for better lubrication). The mixing process was carried out for 2 hours in a Y-type mixer. The test specimens were cylinders with a diameter of d = 12.7 mm, made in three versions of the relative density: ρ_{w1} =0.75; ρ_{w2} =0.80; ρ_{w3} =0.85. For all the specimens variants of different densities, the same weighted amounts were made. The cylindrical specimen shapes had the approximate dimensions d=12.7mm (diameter), and h=12.7mm (height) for the density ρ_{w3} =0.85. The consolidation process was carried out under the conditions of excess pressure of the press, and with the use of distance pieces to obtain the appropriate heights of test specimens of the finished sinters with desired densities. The sintering process was carried out **in H_2 reducing atmosphere at a drew point of -30°C, ensuring reduction of oxides**. The test specimens were preheated at 500°C (for 1 hour), and then sintered at 1100°C (for 45 min). **The use of costly pure hydrogen atmosphere during cooling (duration of 50 min.) has been eliminated by applying a cheaper H_2-N_2 one, composed of** 95% N_2 + 5% H_2. **Small hydrogen addition means low cost and good reduction properties of the atmosphere used.** In order to ensure effective transmission of oscillatory motion of the tools on the material of the test specimens during unconstrained compression, suitable grippable ends were made [12]. The version of the geometry of the test specimen fitted with grippable ends is shown in Fig. 1. Table 3 lists the parameters of the sintered test specimens.

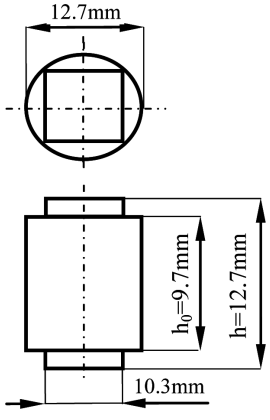

Fig. 1. Geometry of test specimens

TABLE 3

Parameters of test specimens

Preset density	0.75	0.80	0.85	ρ_w
	5.85 [g/cm^3]	6.24 [g/cm^3]	6.63 [g/cm^3]	ρ
Post-consolidation density [g/cm^3]	5.86	6.24	6.63	ρ
Height of test specimens [mm]	14.484	13.645	12.796	after consolidation
	14.430	13.520	12.720	after sintering
Diameter of test specimens [mm]	12.706	12.714	12.727	after consolidation
	12.690	12.700	12.710	after sintering
Mass of sinters [g]	10.710	10.709	10.708	Average values of 10 random test specimens (lot of 80 pcs)
Density of fabricated sinters [g/cm^3]	5.870	6.253	6.635	
Relative density of fabricated sinters	0.747	0.796	0.845	

2.3. Description of deformation conditions

The sintered test specimens were subject to pressed deformation analogous as in case of the unconstrained compression test (as a typical, conventional method used in deformation of both solid and sintered materials). In order to achieve greater uniformity of the parameters of the internal structure (more efficient effect of consolidation homogeneity), a combination of compression and oscillatory torsion was used. There was observed a creation of barrel-shaped cylinders after deformation, being characteristic for the effect of deformation heterogeneity in local areas under conditions of unconstrained compression. The application of the supplementary oscillatory torsion during the compression test allowed the material to follow additional deformation patterns, thereby reducing the heterogeneity of deformation in local areas in solid materials – the effect to be utilised to create favourable conditions for homogeneous consolidation of sinters.

The tests were carried using a test stand allowing the deformation under uniaxial compression combined with torsion. The kinematic diagram of the test stand is shown in Fig. 2.

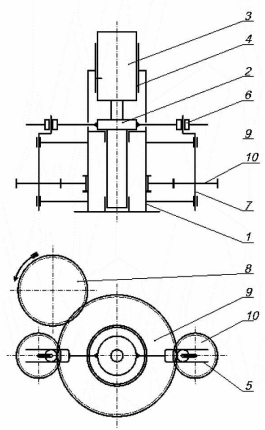

Fig. 2. Kinematic diagram of the combined compression and oscillatory torsion test stand (1. Body, 2. Bottom punch, 3. Upper punch, 4. Non-rotational sliding bearing, 5. Yoke - arm of lower punch, 6. Roll, 7. Crankshaft (eccentric), 8. Driving sprocket, 9. Toothed ring, 10. Toothed gear)

The test stand enables the deformation testing of metallic materials under following conditions:

- conventional compression under different friction conditions, for example, frictionless compression, dry friction compression,
- conventional compression in a locked die, with the possibility of adjustable radial flow of metal,
- oscillatory torsion (no axial motion of the upper punch),
- compression combined with oscillatory torsion under high quasi-hydrostatic pressure conditions.

The deformation path can be adjusted by modifying the share (in the total distortion) of the following components: linear deformations caused by the plane motion of the punch, and non-dilatational strains due to the torsional motion of the punch.

During the tests of deformation of the material there were recorded the time-dependent parameters of the measuring system. Fig. 3 is the schematic diagram of the measuring system. The system enabled to adjust the velocity of the bottom punch v (up to 0.6 mm/s), whilst the permissible compression force F developed within the system was 300 kN. The force parameters i.e. the compression force F, the torsional moment Ms and these of generalized displacement (the deformation path Δh, torsion angle α), were recorded using a general-purpose computer system.

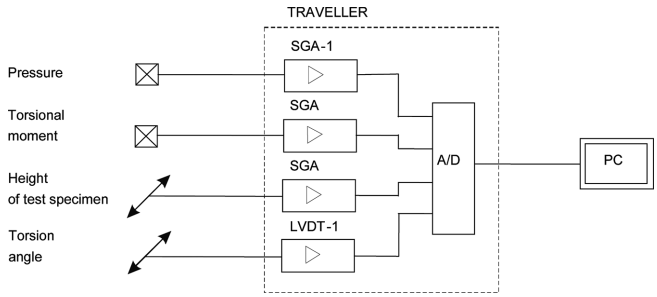

Fig. 3. Schematic diagram of the measuring system employed in the investigations

Fig. 4 illustrates the test stand for deformation of materials under unconstrained compression combined with oscil-

latory torsion. A set of tools used in the basic tests ensuring effective transmission of the oscillatory-torsional motion on the deformation path is shown in Fig. 5.

Fig. 4. The deformation test stand

a.) lower punch.

b.) upper punch

Fig. 5. Tools used in the deformation tests

The tests of unconstrained compression combined with reversible torsion were carried out at the linear velocity of the punches υ =0.1[mm/s]. Three values of the reversible torsion angle were used: $\alpha_{A1} = \pm 3°$; $\alpha_{A2} = \pm 5°$; $\alpha_{A3} = \pm 7°$, respectively. At the given value of $\alpha_{A,}$ the sinters were subject to deformation at three values of torsion frequency: f_1 = 1[Hz]; f_2 = 0.71; f_3 = 0.32, respectively. Table 4 lists the parameters of the deformation tests and the identification numbering of the test specimens:

TABLE 4

Deformation test parameters and the identification numbering of the test specimens

Relative density of sinters prior to deformation	**1 ρ_w = 0.75**								
Test specimen identification number	**1**			**2**			**3**		
Reversible torsion angle	±3°	±3°	±3°	±5°	±5°	±5°	±7°	±7°	±7°
Test specimen identification number	**1**	**2**	**3**	**1**	**2**	**3**	**1**	**2**	**3**
Frequency of reversible torsion cycles f[Hz]	1.0	0.71	0.32	1,00	0.71	0.32	1,00	0.71	0.32

2.4. Determination of the density of sinters

The average density of the sinters for typical solids can be determined directly by dividing the mass by the volume calculated from geometric dimensions. In the case of test specimens with complex geometries it is difficult to determine their volume. So, a hydrostatic weighing method was employed to determine the value of the average density of the post-deformation sinters. There were determined: the weight of the test specimens m_p in air, then the mass m_w of the test specimens immersed in liquid (e.g. in water; adequate care was taken to avoid creation of air bubbles on the surface of the test specimen). The density of the sinter was determined from the following relationship:

$$\rho = \frac{m_p}{m_p - m_w} \rho_w \, [\, g / cm^3 \,] \tag{1}$$

where: ρ – density of the sinter [g/cm^3]

m_p – dry mass of the test specimen weighed in air [g]

m_w – mass of the test specimen immersed in liquid (e.g. in water) [g]

ρ_w – density of the liquid (e.g. water) [g/cm^3]

The calculation took into account the negligence of the grippable ends of the test specimens. Thus, the equation (1) neglecting the grippable ends assumes the following form:

$$\rho_s = \frac{m_c - m_u}{\frac{m_c - m_{wH2O}}{\rho_{H2O}} - V_u} \tag{2}$$

where:

m_c – mass of the whole test specimen weighed in air [g]

m_u – mass of the grippable ends of the test specimen [g]

m_{wH2O} – mass of the test specimen immersed in water [g]

ρ_{H2O} – water density [g/cm^3]

V_u – volume of the grippable ends [cm^3]

In using this method, caution should be taken by investigators to protect pores against water penetration during the weighing of the sinters immersed in the liquid. The details of the density testing of sintered materials are given in DIN 30911, Part 3.

3. The results of investigations

There was determined the density of the sintered test specimens before the deformation, of the sintered test specimens subject to deformation under conditions of unconstrained compression, and of the test specimens subject to deformation under conditions of unconstrained compression combined with oscillatory torsion. Graphs 6, 7, 8 illustrate the test results obtained for variants of sinters with varying initial density.

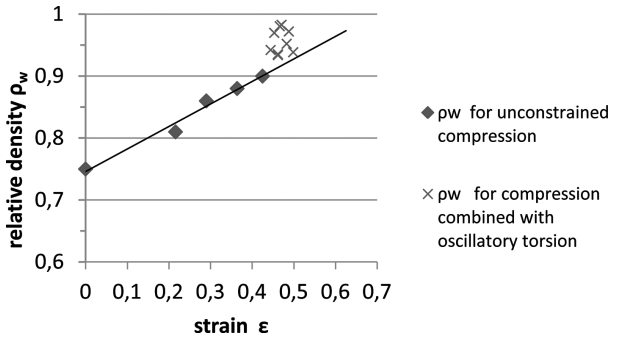

Fig. 6. Relative density of sinters ρ_w tested under conditions of unconstrained compression and after the compression combined with oscillatory torsion. The density of the sinters prior to deformation ρ_w =0.75

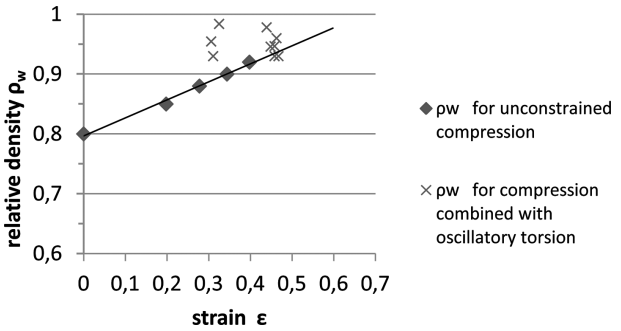

Fig. 7. Relative density of sinters ρ_w tested under conditions of unconstrained compression and after the compression combined with oscillatory torsion. The density of the sinters prior to deformation ρ_w =0.80

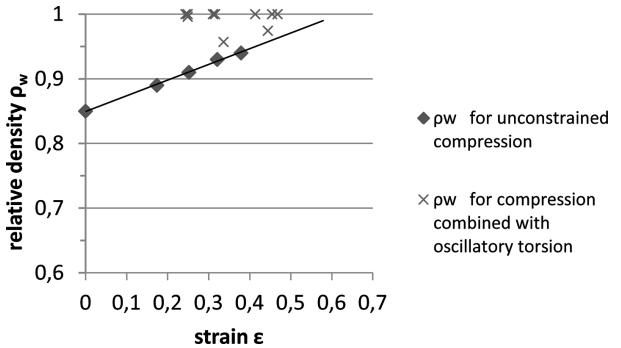

Fig. 8. Relative density of sinters ρ_w tested under conditions of unconstrained compression and after the compression combined with oscillatory torsion. The density of the sinters prior to deformation ρ_w =0.85

It was found, that the application of oscillatory motion of the punches allowed to obtain, for each variant of the initial density of the sinters, the values of average density much higher than those obtained under the unconstrained compression only (Fig. 9, 10, 11). The sinters with higher initial density ρ_w after deformation in complex loading states had the density values similar to those of solid material, but obtained at much lower values of strain ε_h (Fig.7,8).

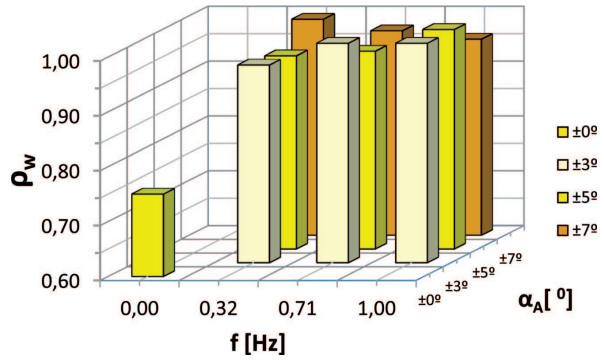

Fig. 9. Value of the relative density ρ_w of the sinters after deformation during the test of unconstrained uniaxial compression combined with oscillatory torsion (in function of the reversible torsion angle α_A and variants of cycle frequency f; the relative density of the sinter prior to deformation ρ_w =**0.75**; the draft attained during the test as in the case of unconstrained compression ε_h ≈**0.45**)

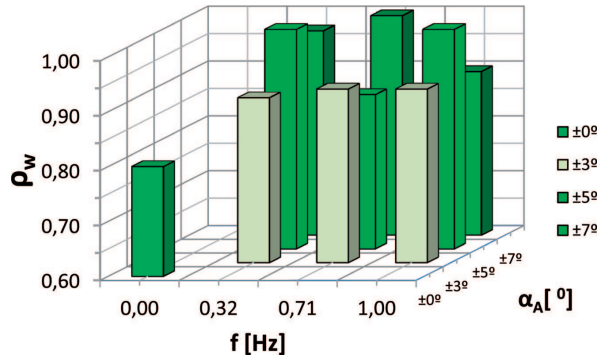

Fig. 10. Value of the relative density ρ_w of the sinters after deformation during the test of unconstrained uniaxial compression combined with oscillatory torsion (in function of the reversible torsion angle α_A and variants of cycle frequency f; the relative density of the sinter prior to deformation ρ_w =**0.80**; the draft attained during the test as in the case of unconstrained compression ε_h ≈0.45; for the series of tests at α_A =±7^0 high densities were obtained at ε_h ≈**0.31**)

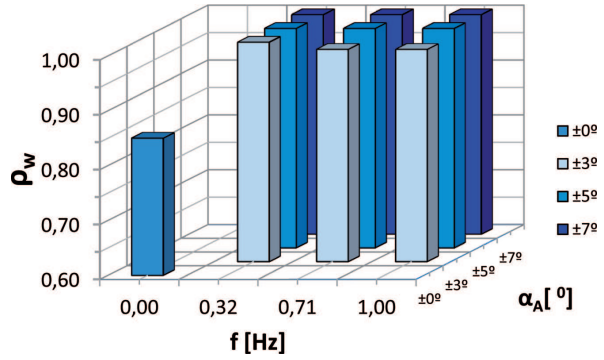

Fig. 11. Value of the relative density ρ_w of the sinters after deformation during the test of unconstrained uniaxial compression combined with oscillatory torsion (in function of the reversible torsion angle α_A and variants of cycle frequency f; the relative density of the sinter prior to deformation ρ_w =**0.85**; the draft attained during the test as in the case of unconstrained compression ε_h ≈0.45; for the series of tests at α_A =±7^0 high values of density were obtained just at ε_h ≈**0.25**)

The homogeneity of density distribution across the sinter volume is an important feature. An indirect method of determination density distribution is to determine the non-uniformity of porosity across the volume of the product. Between the relative density ρ_w and the porosity Θ there is a direct relationship given by the formula (3).

$$\rho_w = 1 - \theta \tag{3}$$

where:

$$\theta = \frac{V_p}{V_c} \tag{4}$$

V_p – total pore volume,

V_c – total volume of the sinter.

Figures 12, 13 are examples of porosity distributions in the sinter having the initial density ρ_w =0.75, and under the conditions of unconstrained compression combined with oscillatory torsion (for selected conditions of oscillatory torsion).

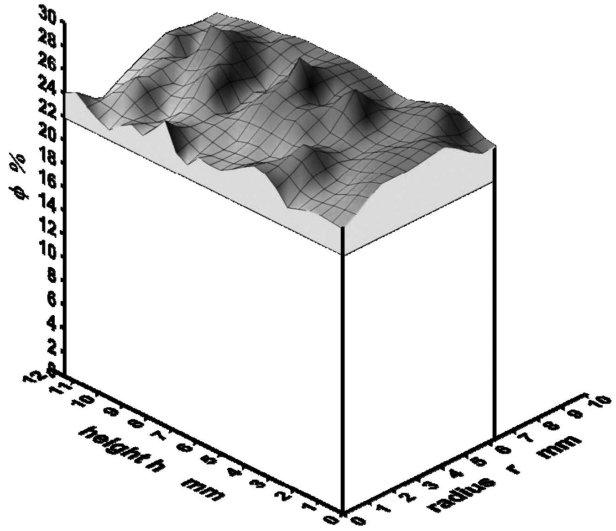

Fig. 12. 3D map of porosity distribution in the sinter having the initial density ρ_w =0.75 (the condition prior to deformation)

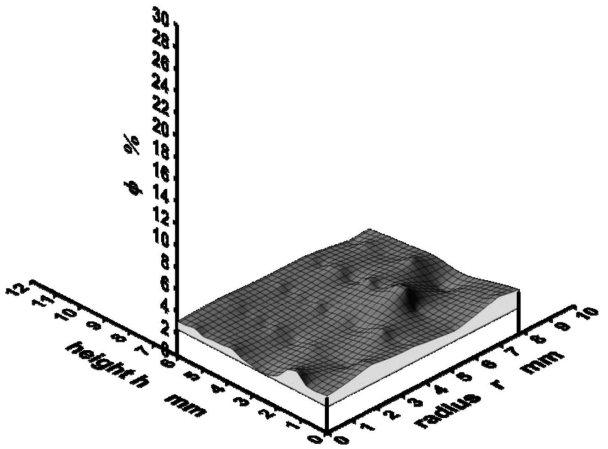

Fig. 13. 3D map of porosity distribution Θ in the sinter having the initial density ρ_w =0.75 subject to deformation under unconstrained compression combined with oscillatory torsion (oscillatory torsion angle $\alpha_A = \pm 5^{0.}$ compression velocity υ =0.1[mm/s], cycle frequency f=0.71[Hz], test specimen No. 1.2.1.)

The local porosity of the test specimens i.e. of the sinters having the initial density ρ_w =0.75 and average porosity φ =25% (fabricated under conditions as for a powder metallurgy operation: single consolidation and sintering) was within the range φ = 22% to φ = 30% (Fig. 12). The porosity of these test specimens was characterised by high heterogeneity in local areas. The deformation of sinters under the conditions like during the uniaxial unconstrained compression provokes an intense increase in density in the central area of the volume of the product, whilst in the direction of radial flow this effect is less intense [7]. It is possible to obtain high, uniformly distributed densities in sinters subject to deformation like in the compression test, but with limited radial flow, what under technological conditions is accomplished using closed dies [6]. The investigations of deformation of sinters under unconstrained compression combined with oscillatory torsion allowed to obtain a high and homogeneous increase of density. Such phenomenon was obtained thorough the introduction of torsion-induced additional deformation during the drafting operation, plus tangential stresses promoting the closing of pores, and resulting in a pattern of little porosity evenly distributed across the volume (Fig.13).

Metallographic studies of the structure of sinters in local areas carried out under deformation conditions used in the tests confirm the efficient and uniform reduction of porosity (Fig.14 and 15 illustrate the results for the chosen deformation scenario).

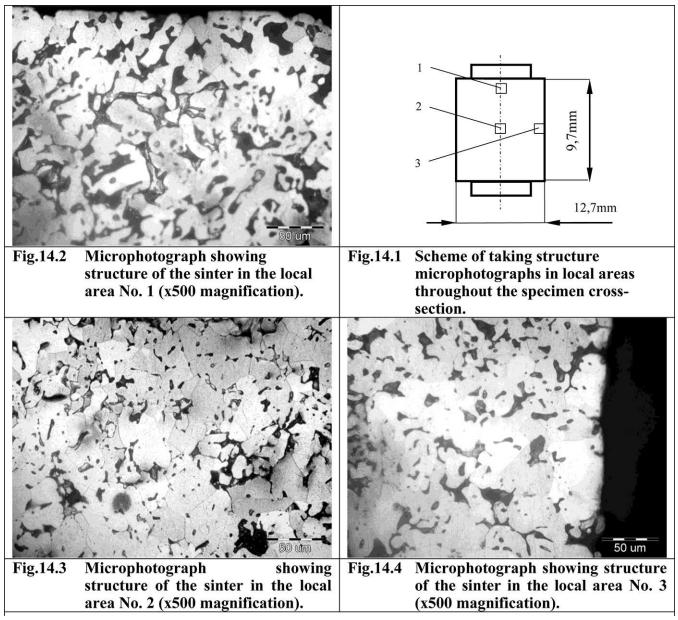

Fig.14.2 Microphotograph showing structure of the sinter in the local area No. 1 (x500 magnification).

Fig.14.1 Scheme of taking structure microphotographs in local areas throughout the specimen cross-section.

Fig.14.3 Microphotograph showing structure of the sinter in the local area No. 2 (x500 magnification).

Fig.14.4 Microphotograph showing structure of the sinter in the local area No. 3 (x500 magnification).

Fig. 14. Metallographic images of the structures in local areas of sintered iron (NC100.24) for the chosen variant having the average relative density ρ_w = 0.75; average porosity ϕ =25% (the condition prior to deformation)

Porosity of sinters produced under conditions corresponding to typical powder metallurgy operations differs considerably in function of local areas and depends upon many factors. One of them is associated with the conditions in which powder compacts are made, as differentiated consolidation is reflected in the porous size and results in a non-uniform distribution of porosity in local areas. Fig.14.2 is a metallographic image showing the structure of the sinter in the local area just beneath the consolidating punch acting on the powder compact. Pores in this area are characterised by a considerable volume

fraction and dramatically irregular shape, like the area where the material contacts the die (Fig.14.4). The middle area is characterised by a very differentiated volume fraction i.e. by the occurrence of zones with high porosity volume fraction, and local low volume fraction spots (Fig.14.3). The application of the combined load conditions during the deformation of sinters – as it has been used in the combined uniaxial compression and oscillatory torsion test – creates the conditions that promote homogeneous consolidation of sinters, by forcing intense and uniform reduction of the size of pores throughout the volume of the product. Fig.15 shows the images of the sinter structure in local areas after deformation (for the chosen deformation scenario) (Fig.13 is the 3D porosity map).

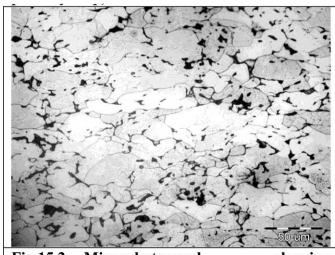

Fig.15.2 Microphotograph showing structure of the sinter in the local area No. 1 (x500 magnification).

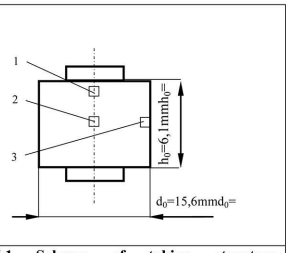

Fig.15.1 Scheme of taking structure microphotographs in local areas throughout the specimen cross-section.

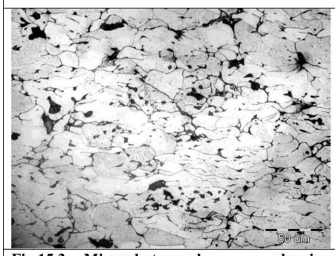

Fig.15.3 Microphotograph showing structure of the sinter in the local area No. 2 (x500 magnification).

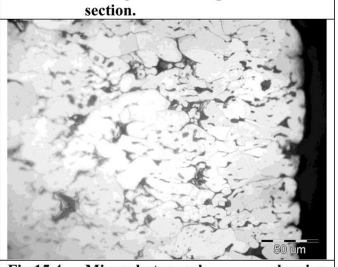

Fig.15.4 Microphotograph showing structure of the sinter in the local area No. 3 (x500 magnification).

Fig. 15. Metallographic images of the structures in local areas of sintered iron (NC100.24) for the situations after deformation under combined load conditions (average relative density prior to deformation $\rho_{\mathbf{w}}$ = 0.75, deformation conditions: oscillatory torsion angle $\alpha_{\mathbf{A}} = \pm 5^0$, compression velocity υ = 0.1[mm/s], cycle frequency f= 0.71[Hz], test specimen No. 1.2.1., average density of the sinter after deformation $\rho_{\mathbf{w}}$ = 0.97, average porosity of the sinter after deformation ϕ = 3%)

There was carried out the analysis of the process of deformation of the sinters under unconstrained compression combined with oscillatory torsion. The deformation was performed in cycles, being dependent on the reverse movement of the punches and the value of the draft per one cycle. In order to provide a thorough description of the deformation, we had to determine both the draft component and that of the torsional motion of the punches in the area, where the deformation behaves proportionally and monotonically. This occurs between the extreme positions of the punch, in the range of the torsion angle from $+\alpha$ to $-\alpha$. Such punch displacement corresponds to the half of the cycle. To describe the process, the components for the proportional and monotonic deformation phases were calculated, followed by the determination of the equivalent deformation for each phase. The results obtained allowed to calculate the value of the cumulative strain ε_{ci} for each phase of the test and for the total cumulative strain ε_c.

The component of deformation produced by the draft during each successive phase was calculated from the formula (5).

$$\varepsilon_{hi} = ln\frac{h_n}{h_{n-1}} \tag{5}$$

where: h_n – height of the sinter after deformation in the specific phase [mm],

h_{n-1} – height of the sinter prior to deformation in the specific phase [mm],

The component of deformation produced by the torsional motion of the punches during each successive proportional and monotonic deformation phase was calculated from the formula (6).

$$\varepsilon_{ski} = \frac{d_{ri}\alpha_A}{2\sqrt{3}h_{ri}} \tag{6}$$

where: $d_{\acute{S}ri}$ – average diameter of the test specimen in the deformation phase [mm],

α_A – total torsion angle between extreme positions [rad],

$h_{\acute{S}ri}$ – average height of the test specimen in the deformation phase [mm].

The equivalent deformation for a given phase of deformation was calculated from the relationship (7).

$$\varepsilon_{zi} = \sqrt{\varepsilon_{hi}^2 + \varepsilon_{ski}^2} \tag{7}$$

where: ε_{zi} – the equivalent strain in the deformation phase.

The cumulative strain for n-th deformation phase was calculated from the relationship (8).

$$\varepsilon_{cn} = \sum_{i=1}^{n} \sqrt{\varepsilon_{hi}^2 + \varepsilon_{ski}^2} \tag{8}$$

$$\varepsilon_{cn} = \sum_{i=1}^{n} \sqrt{\left(ln\left(\frac{h_n}{h_{n-1}}\right)\right)^2 + \left(\frac{d_{ri}\alpha_A}{2\sqrt{3}h_{ri}}\right)^2} \tag{9}$$

Figures 16-18 are the examples of the change of the strain components and the increase of the value of the cumulative strain for the conditions of deformation of the sinter having the initial density ρ_w =0.75.

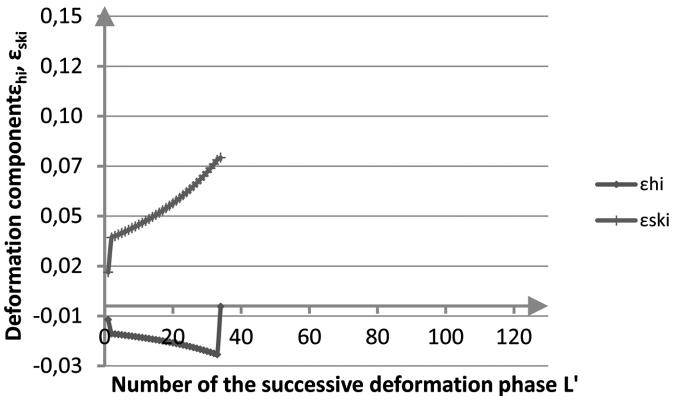

Fig.16.a. Change of the strain components ε_{hi} (draft-induced) and ε_{ski} (torsion-induced) for the individual deformation phases L' (the conditions for the reversible motion of the punches $\alpha_A = \pm 3^{0.}$ f=0.32[Hz])

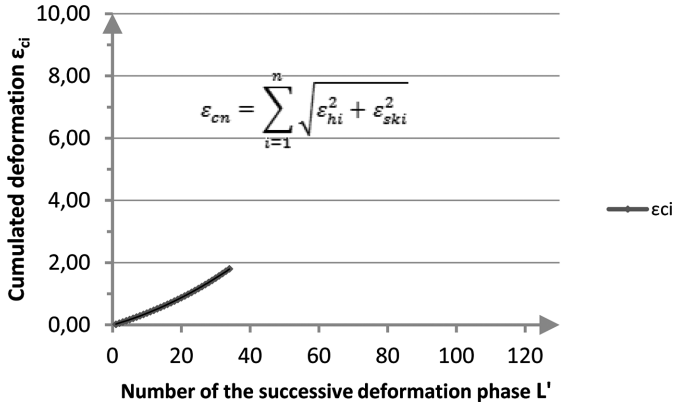

Fig. 16.b. Change of the values of the cumulative strain ε_{ci} during the successive deformation phases (the conditions for the reversible motion of the punches $\alpha_A = \pm 3^{0.}$ f=0.32[Hz])

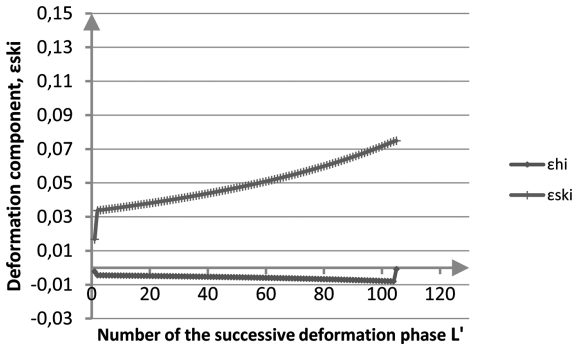

Fig.17.a. Change of the strain components ε_{hi} (draft-induced) and ε_{ski} (torsion-induced) for the individual deformation phases L' (the conditions for the reversible motion of the punches $\alpha_A = \pm 3^{0.}$ f=1[Hz])

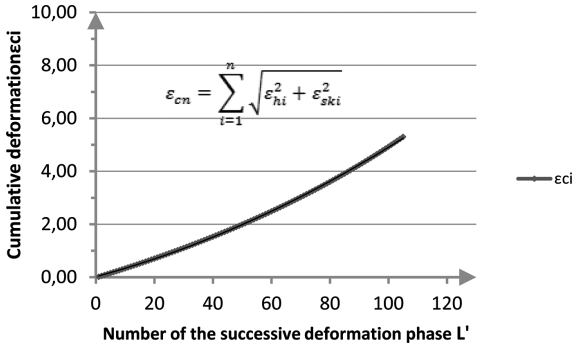

Fig. 17.b. Change of the values of the cumulative strain ε_{ci} during the successive deformation phases (the conditions for the reversible motion of the punches $\alpha_A = \pm 3^{0.}$ f=1[Hz])

The torsion-induced component ε_{ski} had the values far greater than the draft-induced component ε_{hi} for each phase of deformation. The greater the cycle frequency, the stronger the influence of the torsion-induced component ε_{ski} on the value of the equivalent strain in the phase. Under the conditions of unconstrained compression combined with oscillatory torsion, the total cumulative strain ε_c is a function of the conditions of the reversible motion of the punches. An increase of the frequency of cycles of torsion L provokes the increase of the forced deformation path, through the increase of the influence of the torsion-induced strain component ε_{ski}, causing an intense increase of the cumulative strain ε_c.

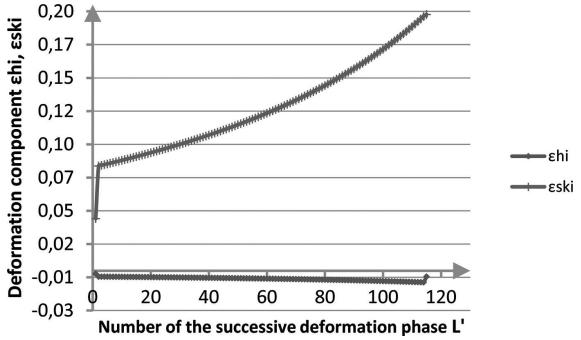

Fig.18.a. Change of the deformation strains ε_{hi} (draft-induced) and ε_{ski} (torsion-induced) for the individual deformation phases L' (the conditions for the reversible motion of the punches $\alpha_A = \pm 7^{0.}$ f=1,0[Hz])

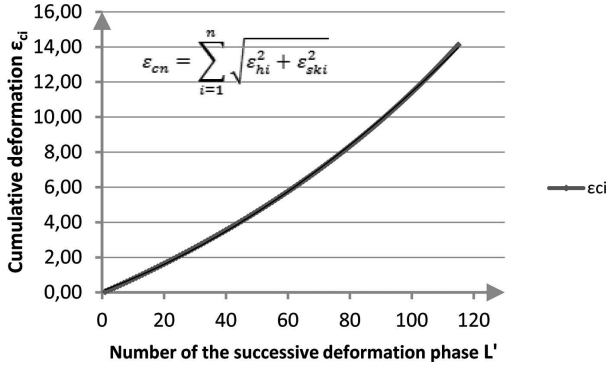

Fig. 18.b. Change of the values of the cumulative strain ε_{ci} during the successive deformation phases (the conditions for the reversible motion of the punches $\alpha_A = \pm 7^{0.}$ f=1,0[Hz])

Fig.18.a illustrates the effect of the increased reversible motion angle α_A on the value of the strain components. The increase of the angle α_A of the reversible motion of the punches during the given phase of deformation (when the deformation changes proportionally and monotonically), significantly affects the lengthening of the deformation path, and thus greatly increases the value of the equivalent strain in that phase, causing an intense increase of the values of the cumulative strain.

Figures19-22 illustrate the change of the value of cumulative strain ε_{cu} at the preset value of the strain ε_h and at the cycle frequency f [Hz] as a function of the angle $\pm\alpha_A$.

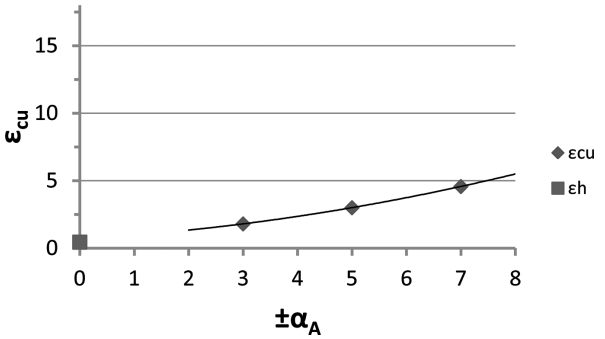

Fig. 19. Values of the cumulative strain ε_{cu} in function of the reverse torsion angle $\pm\alpha_A$ (f=0.32[Hz], υ =0.1[mm/s], $\varepsilon_h \approx 0.45$ at the value of draft as in case of the unconstrained compression test)

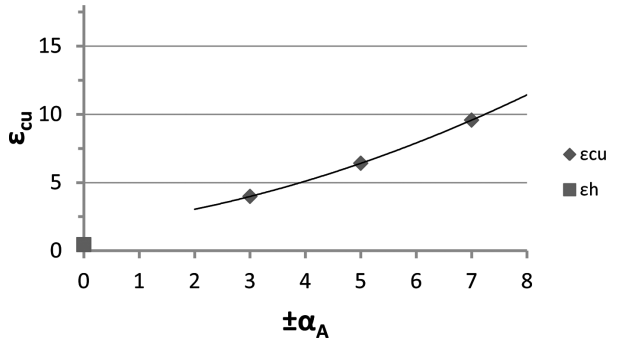

Fig. 20. Values of the cumulative strain ε_{cu} in function of the reverse torsion angle $\pm\alpha_A$ (f=0.71[Hz], υ =0.1[mm/s], ε_h ≈0.45 at the value of draft as in case of the unconstrained compression test)

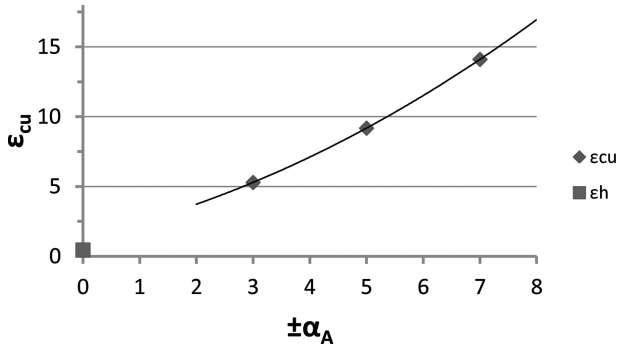

Fig. 21. Values of the cumulative strain ε_{cu} in function of the reverse torsion angle $\pm\alpha_A$ (sinters having the initial density, f=1,0[Hz], υ =0.1[mm/s], ε_h ≈0.45 at the value of draft as in case of the unconstrained compression test)

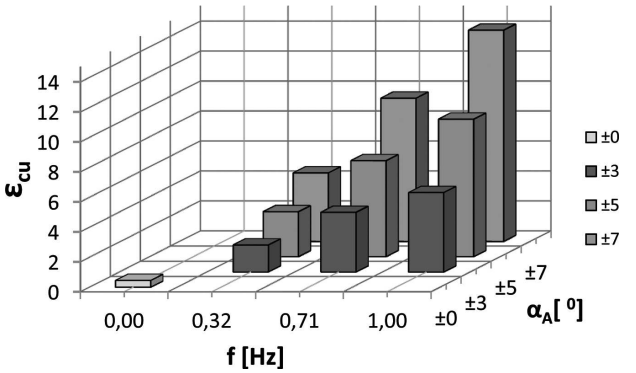

Fig. 22. Values of the cumulative strain ε_{cu} in function of the reverse torsion angle $\pm\alpha_A$ and the torsion cycle frequency f (υ =0.1[mm/s], ε_h ≈0.45 at the value of draft as in case of the unconstrained compression test)

It was observed that under the conditions of our investigations, the increase of the number of cycles had a greater influence on the considerable lengthening of the deformation path, than the change of the angle of the reversible motion of the punches. After deformation, the test specimens had no barrelling, which is characteristic for materials subject to unconstrained compression. Application of oscillatory torsion in the test to unconstrained compression intensifies the process of consolidation of the sinters at the given draft values more efficiently than in the case of the traditional unconstrained upset forging. The distribution of density in local areas after deformation in a complex loading state is uniform and very advantageous due to the effectiveness of the consolidation. The most favourable conditions for consolidation of sinters under the conditions of unconstrained compression combined with oscillatory torsion are associated with the use of smaller angles of the reversible motion of the punches and higher frequencies of the torsional cycles.

4. Summary

The material of the sinter subject to deformation under unconstrained compression combined with oscillatory torsion is subject to consolidation depending on the conditions of the draft and the additional deformation induced by the reverse torsion. It was observed during the whole test, that the deformation was influenced by both the draft-induced component and the component of the reversible motion of the punches. The deformation process was carried out in sequential cycles, where the intensity of the effect of the oscillatory torsion-induced component varies in function of the reversible torsion angle α_A and the cycle frequency f, and is many times greater than the effect of the draft-induced deformation component.

5. Conclusions

- The magnitude of the cumulative strain ε_{cu} is greater, the greater are the parameters of the oscillatory torsion, namely α_A, f, ε_h, and it decreases with the increasing velocity υ.
- The cumulative strain of the material subject to the test of uniaxial unconstrained compression combined with oscillatory torsion enhances the consolidation of the sinters for all variants of deformation parameters α_A and f at the given value of the draft. This effect is more pronounced than in the case of the compression only.
- In order to ensure effective consolidation of sinters with smaller initial densities, small torsion angles be used; on contrary - sinters with higher initial densities would require larger torsion angles.
- It was observed during the deformation of the sinters conducted under the conditions of uniaxial compression combined with oscillatory torsion that the torsion-induced component produced greater effect on the effective consolidation.
- The angle of the reversible motion of the punches α_A is the decisive parameter for the intensity of the increase of the indicator of cumulative strain, while the frequency f affects the change of the number of the deformation phases.
- Sinters with higher initial densities subject to the process of uniaxial unconstrained compression combined with oscillatory torsion require smaller values of the draft ε_h to obtain an efficient (high and uniform) consolidation.

REFERENCES

[1] J. Pawlicki, F. Grosman, Analiza efektów siłowo-energetycznych dla procesów z wymuszoną drogą

odkształcenia, Rudy i Metale Nieżelazne **10-11**, 479-483 (2003).
[2] R. S z y n d l e r, Spęczanie w warunkach zmiennej drogi deformacji, Rudy i Metale Nieżelazne **40**, 11, 482-486 (1995).
[3] J. P a w l i c k i, F. G r o s m a n, Niekonwencjonalne sposoby odkształcania plastycznego materiałów metalicznych, FORMING 2004, Plasticita materialov, 198-203.
[4] F. G r o s m a n, J. P a w l i c k i, Nowe możliwości procesów obróbki plastycznej w warunkach wymuszonej drogi odkształcenia, Hutnik **72**, 5, 280-284 (2005).
[5] A. B e l y a k o v, K. T s u z a k i, H. M i u r a, T. S a k a i, Effect of initial microstructures on grain refinement in a stainless steel by large strain deformation, Acta Materialia **51**, 3, 847-861 February 2003.
[6] M. R o s i a k, F. G r o s m a n, Porowatość w spiekach odkształconych plastycznie na zimno. Zeszyty Naukowe Politechniki Opolskiej **290**, Mechanika 76, 305-309 (2003).
[7] M. R o s i a k, F. G r o s m a n, Zmiany w budowie wewnętrznej spieków odkształcanych na zimno z możliwością nieograniczonego płynięcia promieniowego, Zeszyty Naukowe Politechniki Opolskiej **321**, Mechanika 89, 77 (2007).
[8] M. R o s i a k, F. G r o s m a n, Gęstość materiałów spiekanych po odkształceniu na zimno. Zeszyty Naukowe Politechniki Opolskiej **288**, Mechanika 75, 211-218 (2002).
[9] M. R o s i a k, Odkształcanie spieków w warunkach złożonych stanach naprężeń, Zeszyty Naukowe Politechniki Opolskiej **332**, Mechanika 95, 57 (2009).
[10] M. R o s i a k, Dobór geometrii narzędzi dla zapewnienia efektywnego przenoszenia ruchu oscylacyjno-skrętnego w czasie realizowanych prób ściskania swobodnego, Zeszyty Naukowe Politechniki Opolskiej **337**, Mechanika 97, 157 (2010).
[11] K. H y o u n g S e o p, Ig H. S u n, L. Y o u n g S h i n, A. D u b r a v i n a, I. A l e x a n d e r, Deformation behaviour of copper during a high pressure torsion process, Journal of Materials Processing Technology **2**, 334 (2003).
[12] H. D y b i e c, Plastic consolidation of metallic powders, Archives of Metallurgy and Materials **52**, 2 (2007).

Received: 20 November 2012.